Available online at www.sciencedirect.com
SCIENCE DIRECT®
Journal of Solid State Chemistry 178 (2005) 2759–2765
JOURNAL OF SOLID STATE CHEMISTRY
www.elsevier.com/locate/jssc

Solution preparation of the amorphous molybdenum oxysulfide $MoOS_2$ and its use for catalysis

Daisy Genuit, Igor Bezverkhyy, Pavel Afanasiev*

Institut de Recherches sur la Catalyse 2, avenue A. Einstein, 69626 Villeurbanne Cédex, France

Received 6 May 2005; received in revised form 10 June 2005; accepted 11 June 2005
Available online 21 July 2005

Abstract

Acid condensation of aqueous $MoO_2S_2^{2-}$ anion yields amorphous $MoOS_2$ oxysulfide. This compound possesses tubular morphology and when freshly precipitated is soluble in polar organics such as acetone and ethanol. The ensemble of characterizations (IR, UV–visible, EXAFS spectroscopy) suggests that it contains cyclic or short linear oligomers of neutral molybdenum (V) oxysulfide $MoOS_2$ core. Thermal decomposition of $MoOS_2$ under inert atmosphere leads to the formation of a mixture of MoO_2 and MoS_2 phases. Promotion of $MoOS_2$ with cobalt followed by sulfidation leads to highly active HDS catalysts.

Keywords: Molybdenum; Oxysulfide; Sulfide; EXAFS; Hydrotreating

1. Introduction

Molybdenum sulfides and oxysulfides present considerable interest for many research fields including enzymes and industrial catalysis. Despite considerable amount of work on their structural chemistry, the oxysulfides are in general less studied than molybdenum oxides or sulfides. However, they may exhibit interesting structures and properties. Thus, recently "molecular wheels", have been synthesized consisting of cycles built from the $Mo_2O_2S_2$ core unit, and one able to incorporate guest species [1,2]. A vast variety of sulfur-bridged molybdenum and tungsten coordination compounds have been described [3] but at the same time no individual solid molybdenum oxysulfides is known. Amorphous molybdenum oxysulfides are supposed to be intermediate products of sulfidation of the industrial hydrotreating catalysts [4], but such compounds have never been isolated and characterized. The existence of the intermediate phase $\{MoOS_2\}$ was postulated but its chemical identity remained unclear [4,5].

Soft chemistry routes using solution reactions of molybdenum sulfides and oxysulfides provide an approach for the preparation of new solids, such as new binary amorphous molybdenum sulfides [6]. Recently we have reported on nonstoichiometric molybdenum oxysulfide materials which produced vesicle-like and tubular precipitates in organic solvents. Being obtained through oxidation of polysulfides, these materials have no defined structure; moreover their stoichiometry is variable [7]. However, the presence of oligomers derived from condensation of molybdenum oxysulfide moieties was clearly established. Meanwhile we looked for a rational preparation technique of individual Mo oxysulfides. Here we report on the solution preparation and characterizations of nearly stoichiometric molybdenum oxysulfide $MoOS_2$.

If thiomolybdates [8–10] are widely used for hydrotreating catalysts preparation, oxothiospecies were never reported as catalysts or catalytic precursors. This paper deals with a preliminary study of the application of $MoO_2S_2^{2-}$ core to obtain dispersed sulfide, possessing

*Corresponding author. Fax: +33 4 72 44 53 99.
E-mail address: afanas@catalyse.univ-lyon1.fr (P. Afanasiev).

0022-4596/$ - see front matter © 2005 Elsevier Inc. All rights reserved.
doi:10.1016/j.jssc.2005.06.016

good catalytic properties in the hydrodesulfurization (HDS) reaction.

2. Experimental

Ammonium oxothiomolybdate $(NH_4)_2MoO_2S_2$ has been prepared according to the literature method [11]. Ammonium thiomonomolybdate $(NH_4)MoS_4$ precursor was obtained by adding at ambient temperature 15 g of $(NH_4)_6Mo_7O_{24}\cdot 4H_2O$ to 200 mL of 20 wt% aqueous solution of $(NH_4)_2S$. The precipitated red crystals were thoroughly washed with ethanol, dried and stored under nitrogen. The identity of the compounds has been verified by means of X-ray diffraction and chemical analysis.

To obtain $MoOS_2$ precipitates, 25 ml of 1 M HCl was added upon rapid stirring to a solution of 2 g of $(NH_4)_2MoO_2S_2$ in 100 ml of distilled water. The brown precipitate formed was filtered and washed with water. Drying of the filtered precipitate under a dry nitrogen flow produced black solid $MoOS_2$-1. Alternatively, after repetitive washing and centrifugation wet $MoOS_2$ precipitate was dissolved in 50 ml of acetone with formation of a dark brown solution which is stable in a closed recipient during several weeks. Drying of this acetone solution under a nitrogen flow yields the black solid with metallic lustre, $MoOS_2$-2.

The X-ray diffraction patterns were obtained on a Bruker diffractometer with Cu$K\alpha$ radiation. The diffractograms were analyzed using the standard JCPDS files. Chemical analyses were realized using the atomic emission method. The ESR spectra were registered at 77 or 298 K using a Varian E9 spectrometer working in the X band. The g values were measured relative to the DPPH reference ($g = 2.0036$). UV–visible diffuse reflectance spectra were measured on a Perkin–Elmer lambda 9 spectrometer, using $BaSO_4$ as a reference. The edge energy of the UV–visible absorption was calculated according to Ref. [12]. IR spectra were measured in KBr disks in air on a BRUKER device. Scanning electron microscopy images were obtained on a Hitachi S800 device. Transmission electron micrographs were obtained on a JEOL 2010 device with accelerating voltage 200 keV. The EXAFS measurements were performed at the Laboratoire d'Utilisation du Rayonnement Electromagnétique (LURE), on the XAS2 spectrometer (line D21). They were carried out at 8 K in the transmission mode at the MoK edge from 19 900 to 21000 eV. The EXAFS data were treated with VIPER [13] and FEFF [14] programs. ESI-MS measurements were performed on a Quattro LC triple-quadrupole mass spectrometer. The sample was directly infused into the MS system by a syringe pump without a column at a flow rate of 3 μL min^{-1} and was analyzed in positive ion mode with an electrospray capillary potential of 3.0 kV and a cone potential of 21 V. Collision-induced dissociation of the protonated molecular ions was carried out with a collision energy of 21 V at an argon collision cell pressure of 4.7×10^{-4} kPa. Thermal analysis has been carried out on a Setaram device under inert gas flow at a heating rate 5 K min^{-1}.

To promote the unsupported oxysulfides samples with Co, cobalt nitrate or acetylacetonate were used. For dry impregnation with $Co(NO_3)_2\cdot 6H_2O$ the salt was dissolved in the appropriate amount of water, the solid was thoroughly mixed with the solution and kept in a closed vessel during 6 h at room temperature. The samples were then dried under N_2 at room temperature and resulfided at 673 K for 4 h under 15% vol. H_2S/H_2 flow (3 L/h) mixture. To promote the samples with Co acetylacetonate, the required amount of acetylacetonate complex (Co/Mo atomic ratio = 0.4) was dissolved in the minimum volume of methanol, then MoS_2 or $MoOS_2$ sample was added and the suspension stirred at room temperature during 48 h. Afterwards, the solid was recovered by filtration and dried under N_2 at room temperature and sulfided.

Catalytic activities for thiophene hydrodesulfurization (HDS) were measured at atmospheric pressure in a fixed-bed flow microreactor. In the temperature range 573–623 K the thiophene conversion was lower than 30% under the conditions used (50 mL/min gas flow, 50–60 mg of catalyst) and the plug-flow reactor model could be used to calculate the rate constant:

$$k = \frac{F}{mC}\ln\frac{1}{1-x},$$

where k is the pseudo-first order rate constant (m^3/g s), F the thiophene molar flow (mol/s), m the catalyst mass (g), C the thiophene molar concentration (mol/m^3) and x the conversion determined after 15 h time on stream.

3. Results and discussion

Addition of hydrochloric acid to the light yellow $(NH_4)_2MoO_2S_2$ aqueous solution leads to the instant formation of a dark precipitate. The increase of color intensity suggests lowering the molybdenum oxidation state from Mo(VI) in the solution to Mo(V) or Mo(IV) in the precipitate due to an internal redox process, as it is typical for the molybdenum sulfide compounds.

According to chemical analysis the dried samples contain (wt.) 45.1% Mo, 32.5% S, 0.3% N for the $MoOS_2$-1 specimen and 46.2% Mo, 32.7% S, 0.1% N for the $MoOS_2$-2 one. The calculated values for the exact $MoOS_2$ stoichiometry are (wt.) 54.5% Mo, 36.4% S, 9.1% O. Chemical composition of the solids corresponds to Mo/S atomic ratios of 2.09 and 2.12. Lower than calculated absolute values of the elements contents are certainly related to the adsorbed moisture

and occluded solvent in these disordered amorphous specimens. However the molybdenum to sulfur ratio is close to that expected from the $MoOS_2$ stoichiometry.

ESI MS gives a noisy spectrum with a broad distribution, having the most intense peaks between 600 and 800 m/z, (namely at 648, 663, 665, 737, 740 and 764). This suggests the presence of different oligomeric species, containing probably from four to six Mo atoms. High noise level and great number of peaks in the spectrum do not allow supposing any individual species to be dominant, but variously polymerized Mo complexes.

Scanning electron microscopy of dried $MoOS_2$ solids shows that they consist of rods and tubules with 1–2 μm length and 200–500 nm diameter (Fig. 1). Formation of tubules has already been reported for the amorphous molybdenum oxysulfide phases obtained by air oxidation of ammonium thiodimolybdate $(NH_4)_2Mo_2S_{12}$ acetone solutions [11]. We supposed then that oligomeric species containing oxothimolybdate core are involved in the formation of this particular morphology. Here again we observe microtubular morphology for a nearly stoichiometric oxysulfide compound, in agreement with our previous hypothesis, but the study of morphology as a function of the preparation parameters is beyond the scope of this work.

Fig. 1. Scanning electron microscopy image of the $MoOS_2$-1 solid.

According to the XRD study, the solids $MoOS_2$-1 and $MoOS_2$-2 are amorphous. Their XRD patterns show several very broad maxima similar to those of amorphous MoS_3 (Fig. 2). The IR spectra of the $MoOS_2$ solids (as exemplified by that of $MoOS_2$-1, Fig. 3a) contain the intense bands at 930 and 820 cm^{-1} characteristic for the Mo═O stretching vibrations in the oxosulfide species [4], whereas much weaker bands at 524 and 430 cm^{-1} can be attributed, respectively, to the S–S and Mo═S stretching. The Mo═O vibrations bands in the oxothiomolybdate precursor salt are at 950 and 850 cm^{-1}. The decrease of the stretching frequency observed after condensation corresponds to the loss of oxygen and the increase of share of coordinated sulfur. Indeed, similar frequencies are observed as in the spectrum of the $(NH_4)_2MoS_3O$ compound, with the stretching Mo═O bands at 930 and 823 cm^{-1} (Fig. 3b).

The UV–visible spectrum of the acetone $MoOS_2$ solution shows no individual bands but a monotonic

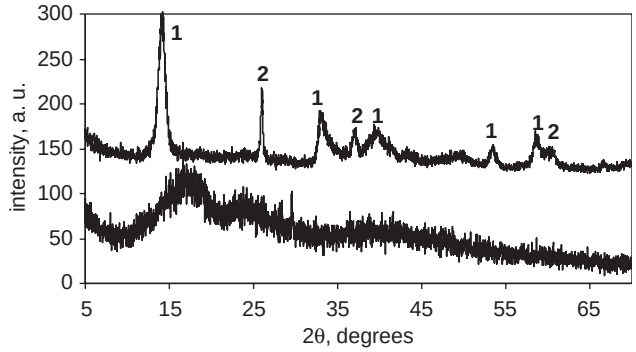

Fig. 2. XRD patterns of the MoOS2-1 solid (bottom pattern) and the same solid after heating at 800 °C in Argon (top pattern). Marks of the peaks: 1-MoS_2 and 2-MoO_2.

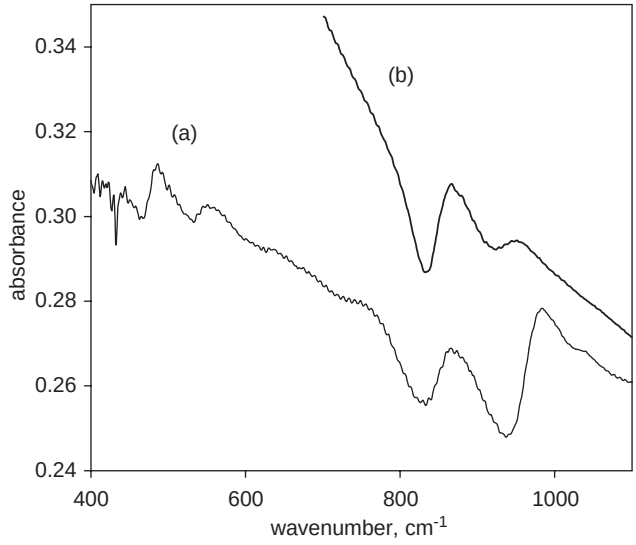

Fig. 3. FT-IR spectra of the $MoOS_2$-1 solid (a) and $(NH_4)_2MoOS_3$ compound (b).

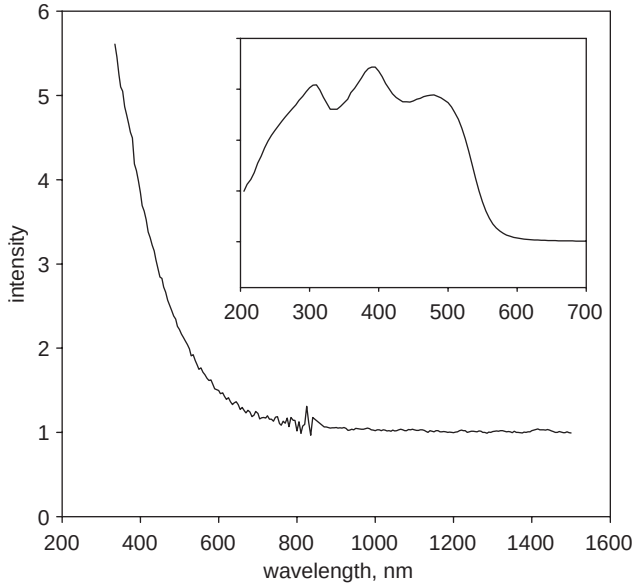

Fig. 4. UV–visible spectrum of the $MoOS_2$ acetone solution. Inset—UV–vis spectrum of the thiooxomolybdate precursor.

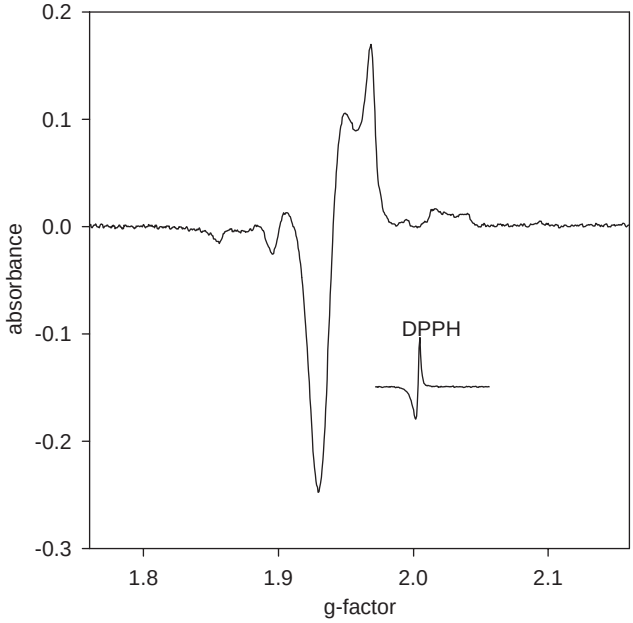

Fig. 5. ESR spectrum of the acetone solution of $MoOS_2$.

decrease of the absorption was towards 600–700 nm (Fig. 4), which corresponds to an energy gap of 2.2 eV between LUMO and HOMO. The spectra observed suggest that the species in the solution are oligomeric, since the individual charge transition bands of the parent monomeric oxothiomolybdate (Fig. 4 insert) have disappeared. In the UV–visible spectra of solid $MoOS_2$ specimens (not shown) continuous strong absorption was observed in the whole wavelength region studied from 200 to 1500 nm.

The ESR spectrum of the $MoOS_2$ acetone solution shows a strong axial signal with a well-resolved hyperfine structure at g factor values lower than 2, characteristic of the oxygen coordinated Mo(V) species (Fig. 5). The ESR parameters of this signal are $g_{y(x)} = 1.965$ $g_{x(y)} = 1.932$ $g_z = 1.896$ $A_\perp = 35$ mT. These parameters are significantly different from those reported for the all-oxygen molybdenyl species [15], probably due to the mixed oxygen–sulfur environment for the Mo(V) centers. When precipitated, the solid still shows an intense ESR signal, but this signal is so strongly broadened that it becomes featureless. Abundant Mo(V) species correspond to the oxidation of sulfur and reduction of molybdenum in the precipitate, presumably due to formation of S–S bonds.

The EXAFS study confirms that in both solid $MoOS_2$ specimens the molybdenum atoms are in mixed oxygen-sulfur environment. Besides, some Mo–Mo bonds are present. Effectively, to obtain a satisfactory fit in both k and r spaces we needed to introduce sulfur, oxygen and molybdenum neighbors in the molybdenum atom environment. Since no constraints on the fitting parameters were imposed (all the four parameters were refined for each shell), the number of neighbors are not integers, but they agree well with the values expected for the $MoOS_2$ polymer. Note that for the parent ammonium salt used as a reference, the coordination sphere of molybdenum was found with greater number of oxygens and smaller number of sulfur ligands, and shorter distances for both ligands (Table 1 and Fig. 6).

Table 1
Mo K edge EXAFS results for the solids $MoOS_2$-1, $MoOS_2$-2 and the parent oxothiomolybdate salt

Atom	R (Å)	N	S (Å^2)	ΔE (eV)
$MoOS_2$-1				
O	1.99	0.8	0.016	−3.7
S	2.42	3.3	0.008	2.5
Mo	2.85	0.7	0.005	8
$MoOS_2$-2				
O	1.97	0.7	0.016	−3.8
O	2.43	3.9	0.008	1.6
Mo	2.82	1.0	0.007	8.2
$(NH_4)_2MoO_2S_2$				
S	1.72	1.7	0.006	−3.1
O	2.21	1.7	0.004	5.5

As concerns the precipitation mechanism, it seems to be analogous to that of thiomolybdate whose acid condensation leads to the chain-like molybdenum trisulfide:

$$MoS_4^{2-} + 2H^+ \rightarrow MoS_3 + H_2S. \quad (1)$$

The ensemble of characterizations indicates unambiguously that the acid condensation of the $MoO_2S_2^{2-}$ species involves formation of water and removal of

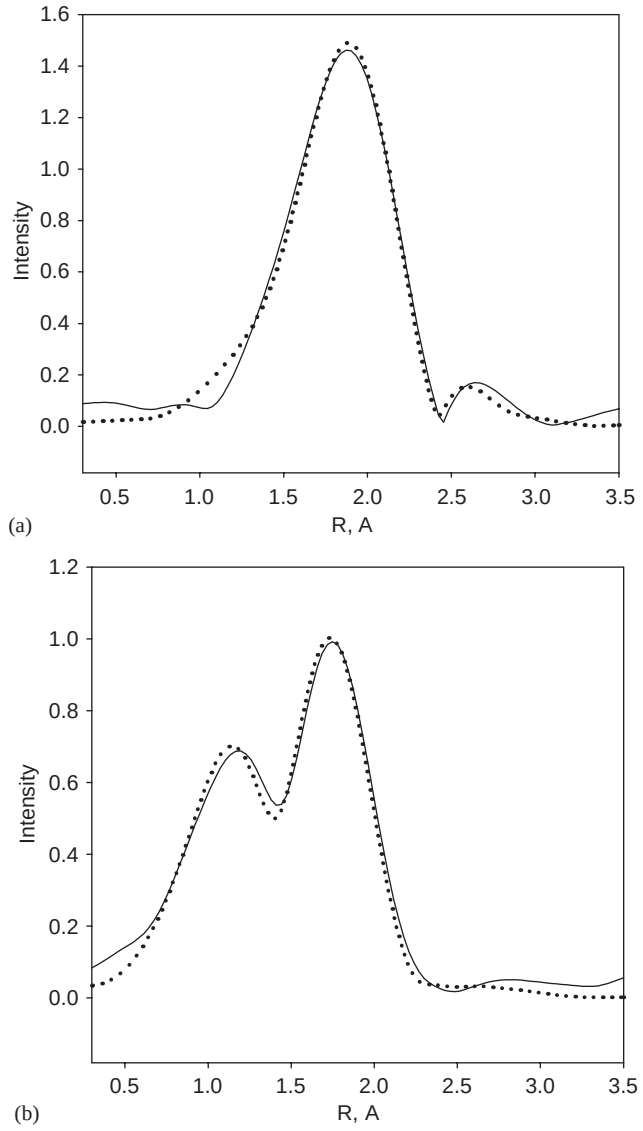

Fig. 6. EXAFS FT transform curves of the spectra of $MoOS_2$-2 solid (a) and the initial $(NH_4)_2MoO_2S_2$ compound (b). Solid curves—experiment, dotted curves—model.

oxygen from the coordination sphere of molybdenum. This is in line with earlier results on the dimerization of this anion upon acidification [16], which also postulate formation of water rather than H_2S:

$$MoO_2S_2^{2-} + 2H^+ \rightarrow MoOS_2 + H_2O. \quad (2)$$

It can thus be thought that the $MoOS_2$ core polymerization involves sharing of the sulfur ligands, probably as follows:

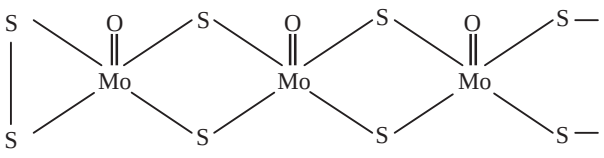

The structure presented above is of course one among many possible others. It is clear that oligomeric species of various compositions are formed in the reaction mixture, but the connection mode seems to be well established.

The solubility of the fresh products in polar organic solvents might be explained by the presence of short linear molecules with terminal disulfur bridges. These molecules are further condensed upon drying or long stay at ambient conditions. This property to give organics soluble precipitate seems to be unique for the $MoO_2S_2^{2-}$ species. When treated with diluted acid, other anions $MoO_xS_y^{2-}$ ($x = 0$, 1, 3) give insoluble amorphous precipitates (our unpublished data).

The reactivity of $MoOS_2$ towards sulfidation and thermal decomposition was briefly studied and compared to that reported for the $\{MoOS_2\}$ solid, the non-clearly defined intermediate of the $(NH_4)_2MoO_2S_2$ thermal decomposition at 200 °C [4]. As expected, sulfidation of $MoOS_2$ with hydrogen sulfide leads very easily (already at 150–200 °C) to dispersed MoS_2 with rather high (though not exceptional) specific surface area of 56 m^2/g as determined by low temperature nitrogen adsorption. It is well known that the sulfidation of molybdenum oxide species is easy and can be accomplished at rather low temperatures [17].

Earlier it was supposed that the $\{MoOS_2\}$ compound decomposes in inert gas with formation of MoS_2 and release of gaseous O_2. Thorough mass spectrometric analysis of the gases produced during thermal decomposition of $MoOS_2$ does not evidence formation of any significant amounts of oxygen or sulfur oxides. Moreover, as follows from the XRD pattern, even if annealed at 800 °C in Argon, the solid consists of mixture MoS_2 and MoO_2 phases, which correspond to the decomposition Reaction (3):

$$2MoOS_2 \rightarrow MoO_2 + MoS_2 + 1/4S_8. \quad (3)$$

Indeed, as follows from the comparison of the elements electronegativity, the release of gaseous oxygen from the thermal decomposition of a metallic oxysulfide seems less probable than oxidation of some sulfur bridges S_2^{2-} to elemental sulfur.

Thermal analysis of the $MoOS_2$ decomposition under inert gas flow (Fig. 7) confirms that decomposition occurs according to Eq. (3). After water elimination (373 K) the mass loss is 16%; the calculated value for Reaction (3) being 18%. Moreover, the principal peak of mass loss and the exothermal event simultaneous with it occurs in the temperature range 693–723 K, near the boiling point of sulfur (719, 6 K). Heat production should be related to the crystallization of MoS_2 and MoO_2 compounds.

The study of sulfided cobalt promoted specimens shows that $MoOS_2$ might serve as an efficient precursor for hydrodesulfurization catalysis. In Table 2, the

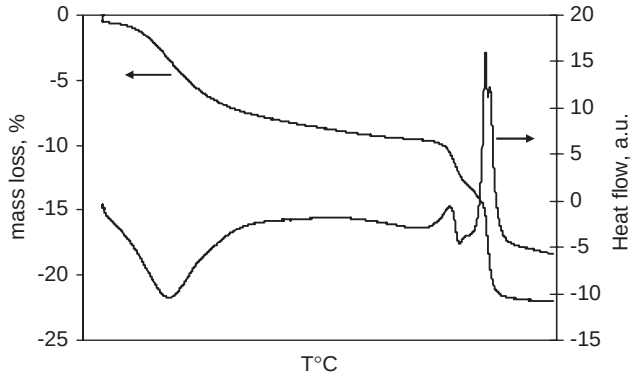

Fig. 7. Thermal analysis of the $MoOS_2$-1 solid unpon its heating under inert gas flow at a rate 5 K min^{-1}.

Table 2
Preparation conditions of unpromoted and cobalt promoted unsupported catalysts, their specific surface areas after HDS test (S) and their steady state HDS activity (A)

Catalyst preparation mode and designation	S, m^2/g after HDS test	A(HDS), 10^{-8} mol/gs 573 K
Ex-thiomolybdate $(NH_4)MoS_4$:MoS_2-I	18	17
Sulfidation product of $MoOS_2$-1: MoS_2-II	20	18
MoS_2-I + Co nitrate: CoMoS-I	34	166
MoS_2-II + Co nitrate: CoMoS-II	32	152
MoS_2-II + Co acac: CoMoS-III	38	211
$MoOS_2$-1 + Co acac: CoMoS-IV	68	270
$CoMo/Al_2O_3$ commercial reference (9% Mo, 3% Co wt.)	220	150

specific surface areas and thiophene HDS catalytic activities of our specimens compared to those of relevant reference compounds which are the product of thiomolybdate decomposition, traditionally used as a reference for the unsupported MoS_2 catalysts (MoS_2-I) and an industrial alumina supported CoMo sulfide catalyst are presented. Obviously the use of $MoOS_2$ to produce unsupported MoS_2 catalyst (MoS_2-II) does not provide any advantage over the oxygen-free $(NH_4)_2MoS_4$ thiomolybdate (MoS_2-I). Promotion of dispersed MoS_2 with cobalt acetylacetonate leads to a considerable increase of activity, in line with previously observed promotion effect [18]. Cobalt nitrate (CoMoS-I, II) promoting leads to lower synergy than the acetylacetonate one (CoMoS-III, IV), presumably because of oxidizing properties of nitrate as discussed in [18]. Again, if cobalt is introduced in the already sulfidized specimens, nearly equal activities are observed for the MoS_4^{2-} -derived and $MoO_2S_2^{2-}$ -solids. The best result is obtained when the dried $MoOS_2$ is directly impregnated with Co acetylacetonate solution and then sulfidized. This leads to a catalyst possessing the highest surface area and HDS activity, possibly due to the particular

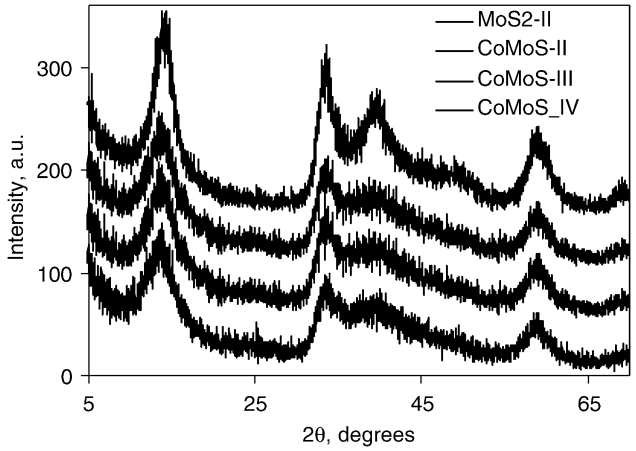

Fig. 8. XRD patterns of the unpromoted MoS_2-II solid and Co pomotedspecimens sulfided at 673 K.

interactions between the cobalt precursor and $MoOS_2$ surface during the impregnation step. Beside the specific surface areas, no significant differences was noted between the sulfided CoMo speciens. At the same time, correlation between the specific surface area and HDS activity is very rough, as can be inferred from Table 2, therefore the differences should be related to fine details of their structure, which at the first sight is very similar. Indeed, chemical composition of all the sulfided solids correcponds to the mixtures of the respective binary sulfides MoS_2 and CoS. The XRD patterns reveal only the presence of dispersed MoS_2 phase (Fig. 8). No cobalt containing phases was observed, indicating that cobalt sulfide entities are smeared over the molybdenum sulfide, probably on the edges of MoS_2 fringes. Lines broadening indicate on high dispersion degree of materials. In agreement with the results of BET surface area measurements, the less crystalline CoMoS-IV has the highest surface area. The EDS assisted transmission miscroscopy shows that the solids consist of highly dispersed MoS_2 with cobalt homogeneously smeared over it. The length of the MoS_2 particle is in the range from 5 to 7 nm and the average number of layers per particle is about 4 (Fig. 9).

In conclusion, this paper reports on the solution synthesis and properties of nearly stoichiometric molybdenum oxysulfide $MoOS_2$. This amorphous solid is soluble in simple organics and possesses original microtubular morphology. It may be of interest for several types of applications. Thus, for example, amorphous thin films of molybdenum and tungsten oxysulfides of similar composition are promising positive electrode materials in microbatteries [19,20]. The oxysulfide described here can easily be supported on any appropriate surface by impregranion and evaporation of its acetone solutions. Another potential application of amorphous $MoOS_2$ concerns the hydrotreating catalysis. Being an organic-soluble and electrically neutral

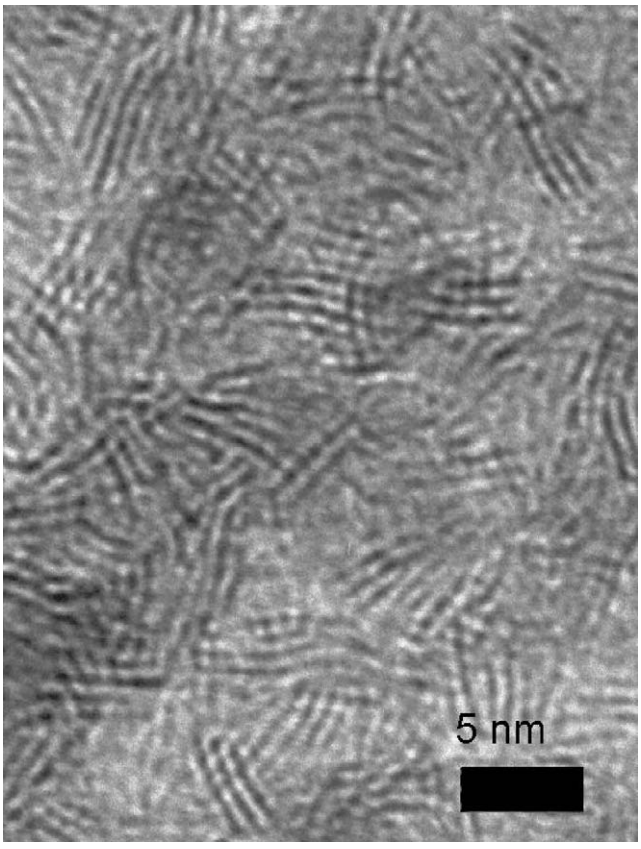

Fig. 9. HRTEM image of the cobalt-promoted $MoOS_2$ sulfided catalyst CoMoS-IV.

precursor, this compound can be a convenient source for introduction of molybdenum sulfide species into small hydrophobic pores, which is the case for example in mesoporous silicas. As for preparation of unsupported catalysts, impregnation of cobalt on freshly dried $MoOS_2$ or on MoS_2 resulting from the $MoOS_2$ sulfidation provides highly active unsupported HDS catalysts.

References

[1] A. Dolbecq, E. Cadot, F. Sécheresse, Chem. Comm. (1998) 2293.
[2] B. Salignac, S. Riedel, A. Dolbecq, F. Secheresse, E. Cadot, J. Am. Chem. Soc. 122 (2000) 10381.
[3] T. Shibahara, Coord. Chem. Rev. 123 (1993) 73.
[4] Th. Weber, J.C. Muijsers, H.M.C. van Wolput, C.P.J. Verhagen, J.W. Niemantsverdriet, J. Phys. Chem. 100 (1996) 14144.
[5] T.P. Prasad, E. Diemann, A. Müller, J. Inorg. Nucl. Chem. 35 (1973) 1895.
[6] P. Afanasiev, I. Bezverkhy, Chem. Mater. 14 (2002) 2826.
[7] P. Afanasiev, I. Bezverkhy, J. Phys. Chem. B 107 (2003) 2678.
[8] G. Alonso, V. Petranovskii, M. Del Valle, J. Cruz-Reyes, A. Licea-Claverie, S. Fuentes, Appl. Catal. A 197 (2000) 87.
[9] G. Alonso, M. Del Valle, J. Cruz-Reyes, A. Licea-Claverie, V. Petranovskii, S. Fuentes. Catal. Lett. 52 (1998) 55.
[10] P. Afanasiev, G.-F. Xia, G. Berhault, B. Jouguet, M. Lacroix, Chem. Mater. 11 (1999) 3216.
[11] J.W. McDonald, G. Delbert Friese, L.D. Rosenhein, W.E. Newton, Inorg. Chim. Acta 72 (1983) 205.
[12] R.S. Weber, J. Catal. 151 (1995) 470.
[13] K.V. Klementiev, J. Synchrotron. Rad. 8 (2001) 270.
[14] J.J. Rehr, S.I. Zabinsky, R.C. Albers, Phys. Rev. Lett. 69 (1992) 3397.
[15] K. Dyrek, M. Labanowska, Colloids Surf. 9 (1984) 385.
[16] W. Rittner, A. Müller, A. Neumann, W. Bäther, R. Chandra Sharma, Angew. Chem. Int. 18 (1979) 530.
[17] R.G. Leliveld, A.J. van Dillen, J.W. Geus, D.C. Koningsberger, J. Catal. 171 (1997) 115.
[18] I. Bezverkhyy, P. Afanasiev, M. Lacroix, J. Catal. 230 (2005) 133.
[19] V. Yufit, M. Nathan, D. Golodnitsky, E. Peled, J. Power Sources 122 (2003) 169.
[20] I. Martin-Litas, P. Vinatier, A. Levasseur, J.C. Dupin, D. Gonbeau, J. Power Sources 97 (2001) 545.